Merging of the polar and tilt instability lines near the respective morphotropic phase boundaries of PbZr$_{1-x}$Ti$_x$O$_3$

F. Cordero,[1] F. Trequattrini,[2] F. Craciun,[1] and C. Galassi[3]

[1]*CNR-ISC, Istituto dei Sistemi Complessi, Area della Ricerca di Roma–Tor Vergata, Via del Fosso del Cavaliere 100, I-00133 Rome, Italy*

[2]*Dipartimento di Fisica, Università di Roma "La Sapienza," P.le A. Moro 2, I-00185 Rome, Italy*

[3]*CNR-ISTEC, Istituto di Scienza e Tecnologia dei Materiali Ceramici, Via Granarolo 64, I-48018 Faenza, Italy*

We present the results of anelastic and dielectric spectroscopy measurements performed on large-grain, ceramic PbZr$_{1-x}$Ti$_x$O$_3$ (PZT) compositions located near the two morphotropic phase boundaries (MPBs) that separate the ferroelectric (FE) rhombohedral (R) phase from the Zr-rich antiferroelectric and Ti-rich FE tetragonal phases. Additional evidence is provided of the existence of a temperature T_{IT}, which we interpret as the onset of the tilt instability in the R phase, where tilting is initially frustrated by lattice disorder but achieves long-range order at the lower temperature T_T. The $T_{IT}(x)$ line is observed for $x < 0.17$, beginning at the $T_T(x)$ line at the point where $T_T(x)$ drops abruptly and then continuing up to the $T_C(x)$ line. If $T_{IT}(x)$ indeed signals the onset of short-range ordered tilting, then it follows that the tilt instability lines should tend to be attracted and merge with those of the polar instabilities. Not only does the $T_{IT}(x)$ line bend toward and then merge with the $T_C(x)$ line but, in our series of samples, the temperature T_{MPB} defined by the dielectric and anelastic maxima at the rhombohedral/tetragonal MPB does not cross the $T_T(x)$ line. Instead it gradually bends downward to become parallel to, and possibly merges with, the $T_T(x)$ line. An abrupt change is found in the shape of the anelastic anomaly at T_T when x passes from 0.465 to 0.48, possibly indicative of a rhombohedral/monoclinic boundary.

I. INTRODUCTION

The phase diagram of the most widely used ferroelectric perovskite PbZr$_{1-x}$Ti$_x$O$_3$ (PZT) still has unclear features (for the phase diagram, see Fig. 7). It has been known since the 1950s[1–3] and the major recent discovery was the existence of a monoclinic (M) phase[4] in a narrow region at the morphotropic phase boundary (MPB) that separates the ferroelectric (FE) Zr-rich rhombohedral (R) region from the Ti-rich tetragonal (T) one. In the M phase the polarization may in principle continuously rotate between the directions in the T and R domains, so providing an additional justification for the well-known and exploited maximum of the electromechanical coupling at the MPB. The existence of domains of the M phase is actually still debated, the alternative being nanotwinned R and/or T domains that over a mesoscopic scale appear as M.[5,6] Since experimental evidences for both types of structures exist, the possibility should be considered that genuine M domains and nanotwinning coexist at the MPB, being both manifestations of a free energy that becomes almost isotropic with respect to the polarization.[7] The part of the MPB line below room temperature has been investigated only after the discovery of the M phase, and is reported to go almost straight to 0 K at $x \simeq 0.52$.[8,9]

Recent studies are also revealing new features of how the TiO$_6$ and ZrO$_6$ octahedra tilt at low temperature. The prediction from first-principles calculations that octahedral tilting occurs also in the M and T phase[10] has been confirmed by anelastic and dielectric,[11] structural,[12] Raman,[13] and infrared[14] experiments. The presence of a low-temperature monoclinic Cc phase[15] with tilt pattern $a^-a^-c^-$ intermediate between tilted R and T has been excluded by a recent neutron diffraction experiment on single crystals,[16] where below T_T coexistence was found of tilted $R3c$ and untilted Cm phases. Yet, evidence for the Cc phase has been subsequently reported on PZT where

6% Pb was substituted with smaller Sr, in order to enhance tilting.[17]

Here we report the results of anelastic and dielectric experiments at additional compositions with respect to our previous investigations,[7,11] which reveal new features of the phase diagram of PZT, and particularly that the lines of the instabilities related to polar modes and octahedral tilting tend to gradually merge with each other rather than to cross.

II. EXPERIMENTAL

Large grain (average sizes 5–30 μm) ceramic samples of PbZr$_{1-x}$Ti$_x$O$_3$, with nominal compositions $x = 0.05$, 0.062, 0.08, 0.12, 0.40, 0.487, 0.494 have been prepared with the mixed-oxide method in the same manner as the previous series of samples.[7,11] The starting oxide powders were calcined at 800 °C for 4 h, pressed into bars and sintered at 1250 °C for 2 h, and packed with PbZrO$_3$ + 5wt% excess ZrO$_2$ to prevent PbO loss during sintering. The powder x-ray diffraction did not reveal any trace of impurity phases and the densities were about 95% of the theoretical ones. The sintered blocks were cut into thin bars 4-cm long and 0.6-mm thick for the anelastic and dielectric experiments and discs with a diameter of 13 mm and a thickness of 0.7 mm were also sintered only for the dielectric measurements. The faces were made conducting with Ag paste.

The dielectric susceptibility $\chi(\omega,T) = \chi' - i\chi''$ was measured with an HP 4194 A impedance bridge with a four-wire probe and an excitation of 0.5 V/mm, between 0.1 and 100 kHz. The heating and cooling runs were made at 0.5–1.5 K/min between 100 and 800 K in a modified Linkam HFS600E-PB4 stage and up to 540 K in a Delta climatic chamber.

The dynamic Young's modulus $E(\omega,T) = E' + iE''$ was measured between 100 and 770 K in vacuum by electrostatically exciting the flexural modes of the bars suspended on thin thermocouple wires.[18] The reciprocal of the Young's modulus, the compliance $s = s' - is'' = 1/E$, is the mechanical analogue of the dielectric susceptibility. During a same run the first three odd flexural vibrations could be excited, whose frequencies are in the ratios 1 : 5.4 : 13.2. The angular frequency of the fundamental resonance is[19] $\omega \propto \sqrt{E'}$, and the temperature variation of the real part of the compliance is given by $s(T)/s_0 \simeq \omega_0^2/\omega^2(T)$, where ω_0 is chosen so that s_0 represents the compliance in the paraelectric phase. The imaginary parts of the susceptibilities contribute to the losses, which are presented as $Q^{-1} = s''/s'$ for the mechanical case and $\tan\delta = \chi''/\chi'$ for the dielectric one.

III. RESULTS

For clarity, we will consider separately the anelastic and dielectric spectra with compositions in the range $0.05 < x < 0.2$, and those in the MPB region. We will present the new data together with those already published in Ref. 11 ($x = 0.455$, 0.465, 0.48, and 0.53) and Ref. 7 ($x = 0.1$, 0.14, 0.17, 0.42, 0.45, 0.452).

A. Octahedral tilting below T_T and T_{IT}: $0.062 < x < 0.2$

Figure 1 presents the dielectric and anelastic spectra measured during heating of $PbZr_{0.92}Ti_{0.08}O_3$, a composition where also the new transition at T_{IT} is clearly visible in the elastic compliance s'. The comparison between the two types of susceptibilities puts in evidence their complementarity in studying combinations of polar and nonpolar modes. The
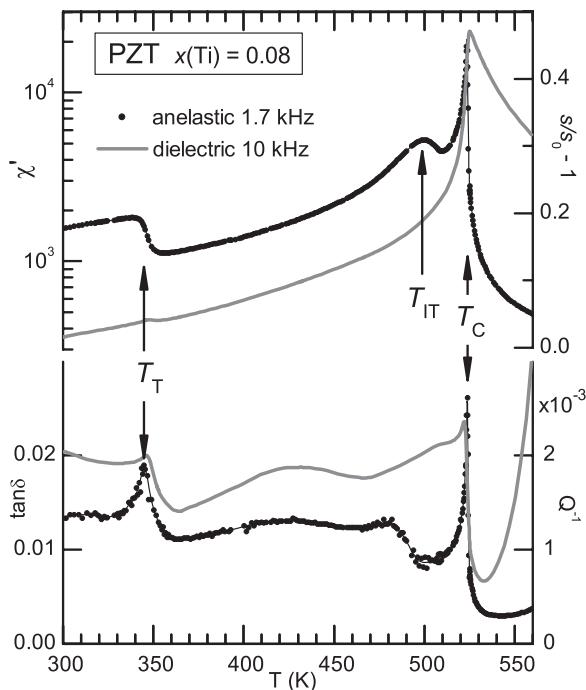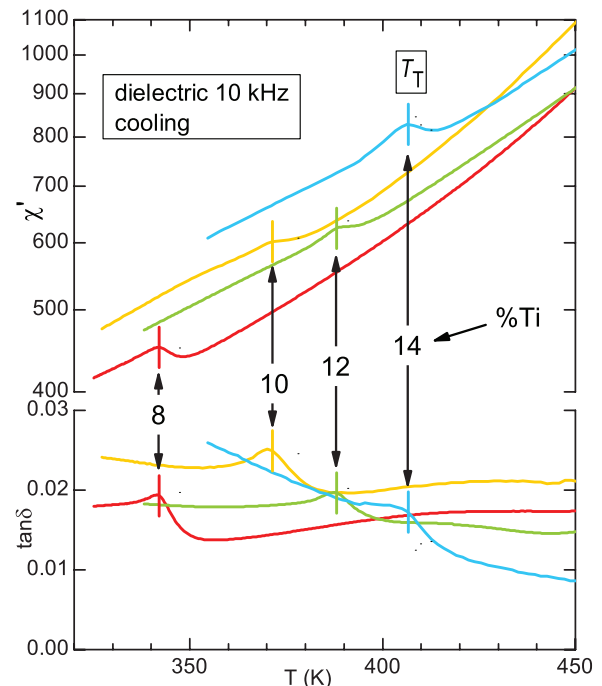

FIG. 2. (Color online) Dielectric susceptibility and loss of $PbZr_{1-x}Ti_xO_3$ measured during cooling through the tilt transition.

dielectric susceptibility χ' is of course dominated by the FE transition at T_C (note the logarithmic scale); it has a very attenuated step below the well-known tilt transition at T_T, and practically nothing visible at T_{IT}, due to both the broader shape of the anomaly and the proximity to the Curie-Weiss peak. The dielectric losses provide an indirect but more clear mark of the nonpolar transition at T_T, presumably through a change in the mobility and/or amplitude of charge and polar relaxations which are affected by octahedral tilting.

The effect of cooling through T_T on the dielectric susceptibility is more convincingly shown to be a positive step in Fig. 2, which should be a sign of cooperative coupling between tilt and polar modes, as discussed more thoroughly elsewhere.[20]

The elastic compliance s', on the other hand, is only indirectly affected by the FE transition, since strain is not an order parameter of the transition and is linearly coupled to the square of the polarization. The Landau theory of phase transitions[21,22] predicts a step in s' for this type of coupling, which is indeed observed at higher Ti compositions,[11] but has a strong peaked component in Zr-rich PZT. We do not have an obvious explanation for this peaked response, which is frequency independent and intrinsic, but mechanisms involving dynamical fluctuations of the order parameter coupled with strain are possible.[22] The advantage of a reduced anelastic response to the FE instabilities is that the other transitions are not as masked as in the dielectric case, so that not only is the tilt transition at T_T clearly visible as a step in s' and peak in Q^{-1}, but also a possible new transition can be detected at T_{IT} even very close to T_C. As already discussed,[7] this anomaly has all the features of the transition at T_T but is spread over a broader temperature range, so providing further support to an explanation in terms of a disordered precursor to the final long-range order (LRO) tilting below T_T.
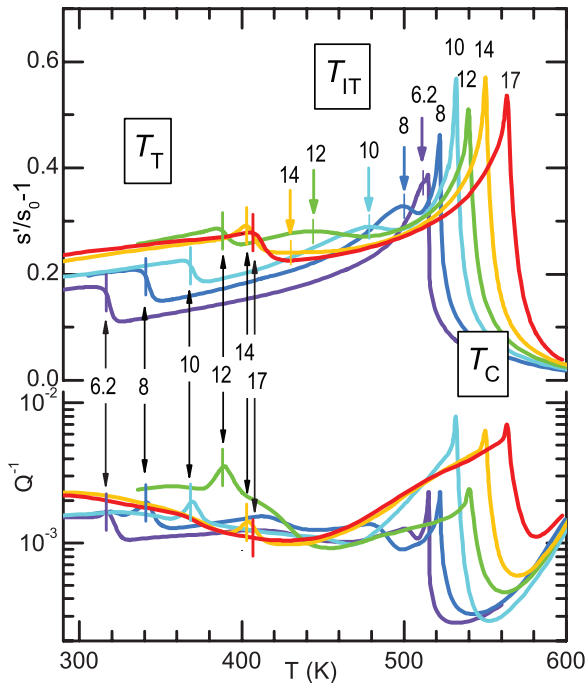

FIG. 1. Dielectric (left ordinates) and anelastic (right ordinates) spectra (higher panel real susceptibilities, lower panel losses) of $PbZr_{0.92}Ti_{0.08}O_3$ measured during heating.

FIG. 3. (Color online) Elastic compliance s' and energy loss coefficient Q^{-1} measured at $\sim$1.7 kHz on PZT at the compositions 6.2, 8, 10, 12, 14, 17% Ti, as indicated by the numbers at the phase transitions. The curves of 10, 14, and 17% Ti are from Ref. 7 .

The broad peaks and steps in both the dielectric and anelastic losses below T_C have shapes and amplitudes that depend on frequency and temperature rate. This indicates their extrinsic origin, namely the motion of domain walls and charged defects, whose state depends on the thermal history. Instead, all the features indicated by arrows are completely independent of the measuring frequency, temperature rate, and thermal history, and therefore are recognizable as intrinsic effects due to the FE and tilt transitions. Hysteresis between heating and cooling is observed due to the first-order character of the transitions and to the presence of domain wall relaxations. Examples of the differences between the features that are intrinsic and stable and those that present dispersion in frequency or are less reproducible have been reported previously[7,11] and are omitted here.

Figure 3 presents the anelastic spectra of PZT with $0.062 < x < 0.17$, including compositions already present in Ref. 7. All the curves are similar to the $x = 0.08$ case of Fig. 1, with the three type of transitions at T_C, T_{IT}, and T_T clearly visible in separate temperature ranges. Both the s' and Q^{-1} curves have sharp peaks at the FE transitions, so that the T_C's are simply labeled with the compositions in %Ti. The other transition temperatures are indicated by vertical bars centered on the curves and arrows labeled with the respective compositions. The features of Q^{-1} in the T_{IT} temperature range are not labeled because they are due to the extrinsic contributions mentioned above.

The temperatures of the tilt transition are identified with the upper edges of the steps in the real parts, which generally coincide with a spike or sharp kink in the losses. The rounded step and lack of reproducible anomaly in the losses increase the error on T_{IT}, which, however, remains small enough to
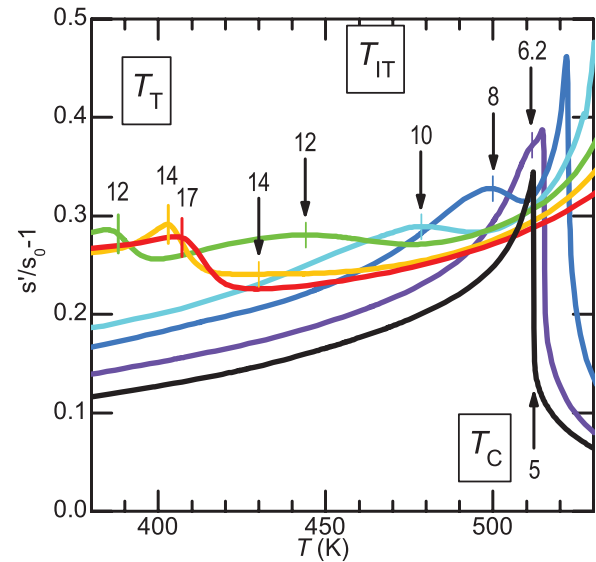

FIG. 4. (Color online) Detail of the anomalies of the elastic compliance at T_{IT}, measured at $\sim$1.7 kHz during cooling on samples with $0.05 \leqslant x \leqslant 0.17$. The numbers indicate the compositions in %Ti. The curves of 10, 14, and 17% Ti are from Ref. 7.

not change the features of the phase diagram discussed later. Due to the importance of the behavior of $T_{IT}(x)$ in Sec. IV, a detail of this anomaly in the $s'(T)$ curves, including 5% Ti, is shown in Fig. 4. A step at T_{IT} is deduced also for $x = 0.14$ by comparison with the $x = 0.17$ case. In this temperature region the two s' curves are nearly coincident, except for the shift of the step at T_T and an additional step in the $x = 0.14$ curve. The broad step deduced from the difference of the two curves fits the trend of the step that defines T_{IT} at lower Ti content, which shifts to lower temperature and broadens with increasing x. A similar anomaly might also be present slightly above T_T for $x = 0.17$, but lacking a clear sign of it, it is assumed to coincide with T_T. At low x, the curve of $x = 0.05$ does not present any clear shoulder below T_C, and it is assumed $T_{IT} \equiv T_C$.

The transition temperatures measured on both heating and cooling are reported in the phase diagram of Fig. 7, where the T_{IT} line departs from T_T at $x \simeq 0.17$, has a kink centered at $x = 0.11$, and finally joins the T_C line at $0.05 < x < 0.062$. The new feature found here is the kink and the merging with T_C at $x > 0.05$. Note also that the anomaly at T_{IT} becomes more intense and sharper on approaching T_C.

B. Compositions near the MPB

As discussed in the previous investigations,[7,11] the MPB in PZT is signaled by a maximum in the dielectric and above all elastic susceptibilities. Again, it is stressed that such maxima are almost independent of frequency and temperature rate, and therefore are intrinsic effects due to the evolution of the order parameter at the MPB and its coupling with strain. In addition, the losses are rather high in the region of the MPB, but no feature is found that is directly ascribable to the phase transition; rather, their dependence on frequency and thermal history show that they are due to the abundant twin walls and other domain boundaries, whose density and mobility depend on many factors and is maximal around the MPB. Instead, the anelastic

losses contain clear cusps or steps at the tilt transitions,[7,11] so allowing T_T to be determined also in the proximity with the MPB, where the real part is dominated by the peak at T_{MPB}. We therefore discuss separately the real parts of χ and s, containing information on the polar transition at the MPB, and the losses, containing information on the tilt transitions.

C. Maxima of the susceptibilities at the MPB

Figure 5 is an overview of χ' and s' curves measured during cooling at all the compositions $x \geqslant 0.40$ we tested so far.

We call T_{MPB} the temperatures of the maxima in χ' and s', marked with vertical bars on the curves. These temperatures do not coincide exactly with each other, because χ' and s' are two different response functions of polarization and strain,
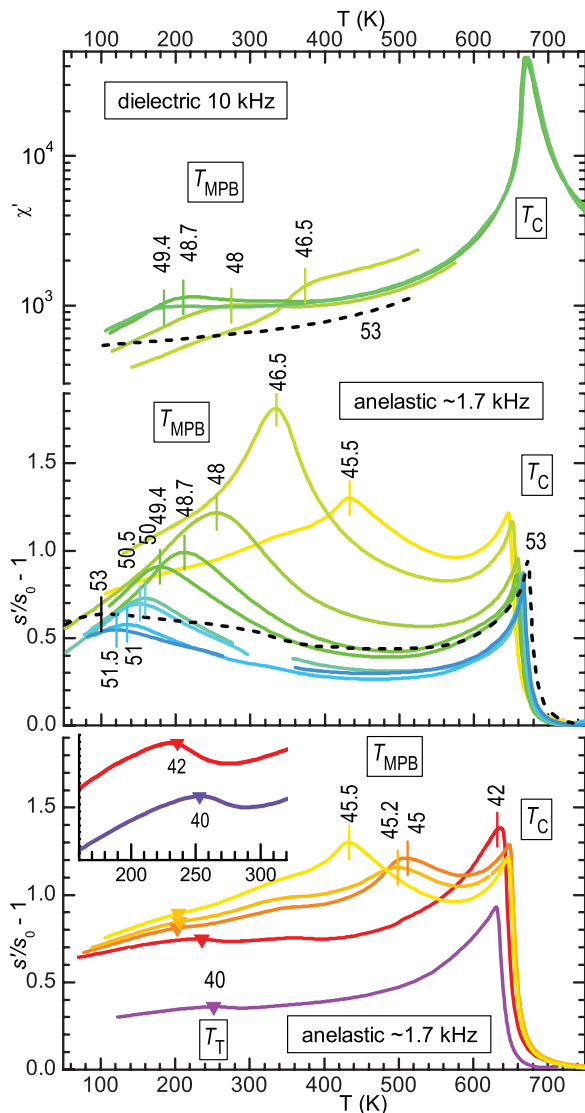

FIG. 5. (Color online) Dielectric susceptibility and elastic compliance measured during cooling on PZT at the compositions indicated besides the curves in % Ti. The T_{MPB}'s are indicated with vertical bars and T_T by triangles (only for $40 \leqslant x \leqslant 45.2$). The inset is an enlargement of the T_T anomalies for 40 and 42% Ti. (Present work) 40, 48.7, and 49.4% Ti; the other curves are from Refs. 7 and 11.

respectively, but, once plotted in the phase diagram, they present an excellent correlation with the MPB determined by diffraction, at least in the middle of the MPB line (see Fig. 7). The dielectric maxima at T_{MPB} are much smaller and broader than the Curie-Weiss peak at T_C (note the logarithmic scale), whereas the anelastic maxima at T_{MPB} have comparable or even larger intensities than the step at T_C (part of the peaked component at T_C has a frequency dispersion denoting relaxation of walls[7,11]).

At $x = 0.40$ there is no peak attributable to the MPB, but only a minor step below T_T, which is indicated with triangles up to $x = 0.452$; beyond that composition, the step at T_T either disappears or is masked by the MPB peak. The other shallow anomaly centered at ~360 K in the curves up to $x \leqslant 0.465$ is the counterpart of the domain wall relaxation appearing in the losses mentioned above and will be ignored. For $x \geqslant 0.45$ the peak at the MPB shifts to lower temperature and develops its maximum amplitude at 0.465, which has been argued to correspond to the point of the phase diagram where the anisotropy of the free energy is minimum.[7]

Beyond $x > 0.465$, the peak at T_{MPB} gradually decreases its amplitude and temperature, and, thanks to the great number of closely spaced compositions, is clearly recognizable as the signature of the MPB up to $x = 0.515$. The next composition, $x = 0.53$ (dashed curves), still has a shallow maximum at a temperature that continues the $T_{MPB}(x)$ line, but its nature appears different. In fact, the dielectric χ' at the same composition lacks any sign of a maximum, and the overall s' curve does not any more continue the trend of the preceding curves. For this reason, the temperature of this maximum at $x = 0.53$ is reported in the phase diagram as T_{MPB} but accompanied by a question mark. A T_{MPB} is extracted also from the curve at $x = 0.42$, even though a separate maximum is not present. It is, however, the only composition where s' has no sharp feature at T_C, and we assume that this is due to a rounded peak at T_{MPB} very close to T_C.

D. Tilt transition near the MPB

For $x > 0.4$ the best signatures of the tilt transition below T_T are found in the anelastic losses. Figure 6 shows the $Q^{-1}(T)$ curves at all the compositions $x \geqslant 0.40$ we tested so far (only 45.2%Ti is omitted in order to not overcrowd the figure).

The T_T's up to $x = 0.455$ are the same as deduced from the step in the real part and are indicated by triangles in Fig. 5. Up to $x = 0.465$ T_T is identified with the temperature of a spike in $Q^{-1}(T)$, which gradually becomes a cusp and starting from $x = 0.48$ becomes a large step. As in the previous figures, the T_T's are marked by vertical bars centered on the curves and joined by a dotted line, in order to better follow the evolution of the anomaly. The transition between the spike/cusp and the step anomaly is unexpectedly sudden, since it occurs within $0.465 < x < 0.48$. Such a discontinuity appears also in the dotted line joining the anomalies, and is marked by an arrow. We emphasize again that the losses generally have a limited reproducibility, because they depend on the status of domain walls and defects; therefore, the regularity of the dotted curve joining the tilt anomalies of so many different samples is remarkable and testifies to the good and uniform quality of the samples.
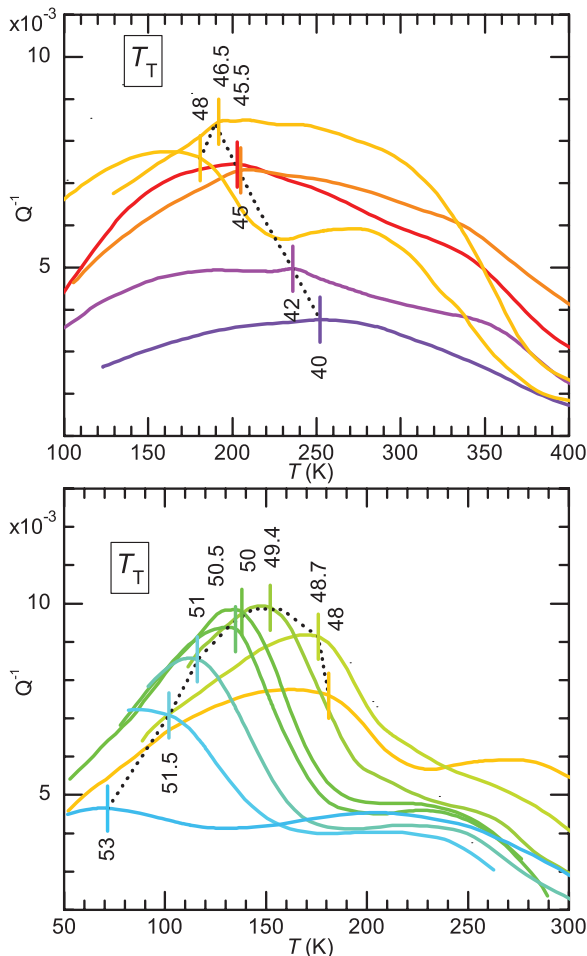
FIG. 6. (Color online) Elastic energy loss coefficient of PZT at the compositions indicated by the numbers (in %Ti), measured during cooling at ~ 1.7 kHz. The anomalies at T_T are indicated by vertical bars and joined with a dotted line. (Present work) 40, 48.7, and 49.4% Ti; the other curves are from Refs. 7 and 11.
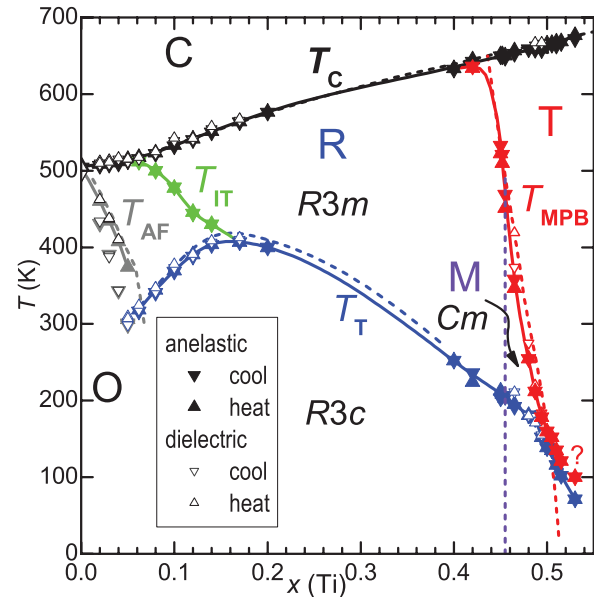

FIG. 7. (Color online) Phase diagram of PZT based on our anelastic and dielectric spectra. The solid lines join the anelastic data measured during heating; the dashed lines are those from Jaffe and Noheda. The question mark reminds that the shallow maximum of s' with $x = 0.53$ at that temperature probably does not signal the MPB crossing.

IV. DISCUSSION

We refer to the phase diagram of PZT in Fig. 7. Below T_C and with decreasing Ti content, one finds the following phases:[23–25] ferroelectric (FE) tetragonal (T) $P4mm$ with polarization **P** along [001], monoclinic (M) Cm with **P** rotated toward $\langle 111 \rangle$, rhombohedral (R) $R3m$ with **P** $\parallel \langle 111 \rangle$, and antiferroelectric (AFE) orthorhombic (O) $Pbam$ with staggered cation shifts along the $\langle 110 \rangle$ and $a^- a^- c^0$ tilt pattern. Below T_T octahedral tilting occurs in all phases.

In Fig. 7, the solid lines join the transition temperatures deduced from our anelastic spectra measured during heating (solid triangles pointing upward), which are generally very close to the points deduced from the dielectric curves (open triangles). The temperatures measured during cooling are also shown as triangles pointing downward. The figure contains all the data presented here and in Refs. 7,11 and, for completeness, also points obtained at compositions $x \leqslant 0.05$, that will be discussed in a future paper. The dashed lines are from the most widely published version of Jaffe *et al.*[3] with modifications of Noheda *et al.*[8] around the MPB.

A. The octahedral tilt instability

The instability of the octahedral network toward tilting is a common phenomenon in perovskites ABO_3, and is usually well accounted for by the mismatch between the network of B-O bonds with that of A-O bonds. When the latter is softer and with larger thermal expansion,[26,27] lowering temperature or increasing the average B size sets the stiff B-O network in compression, which is relieved by octahedral tilting.[25,28–30] This is the case of zirconates and titanates, and generally of perovskites where B has higher valence than A, which can be rationalized in terms of the bond valence sum concept.[31] In the case of PZT, Zr has a radius 19% smaller than Ti and one expects the tilt instability to occur below a $T_T(x)$ line that encloses the low-T and low-x corner of the $x - T$ phase diagram. Indeed, the Zr-rich antiferroelectric compositions are tilted ($a^- a^- c^0$ in Glazer's notation,[32] meaning rotations of the same angle about two pseudocubic axes in antiphase along each of them and no rotation around the third axis), below a $T_{AF}(x)$ line that goes steeply toward 0 K at $x \sim 0.05$ (Fig. 7). In addition, at higher Ti compositions tilting is observed ($a^- a^- a^-$ compatible with the rhombohedral $R3c$ structure) below a T_T line that presents a maximum at $x \sim 0.16$ and whose continuation to low temperature was not followed beyond $x = 0.4$ until recently.[10,11] There is also an earlier report of the tilted T phase based on the electron and neutron diffraction, though the transition temperatures did not appear as continuations of the T_T line.[33,34] It turns out, therefore, that the region of tilted phases has a deep depression at the MPB between the AFE and FE phases, that has been explained in terms of frustration of AFE displacements of the Pb ions perpendicularly to the average FE direction $\langle 111 \rangle$. Such displacements lack the LRO of the AFE-O structure, and

their frustration would be transmitted to the octahedral tilting through the Pb-O bonds, so lowering the T_T border in proximity with the AFE-O phase.[25] Certainly the sharp depression in the border to the LRO tilts, the $T_{AF} + T_T$ line, appears to be caused by some kind of frustration, but it is our opinion that while cation disorder may well hinder the formation of tilt patterns with LRO, it cannot prevent the relieving of the mismatch between B-O and A-O networks. The only manner in which this is accomplished is through octahedral rotations, the only normal modes of a cubic perovskite that induce a decrease of the ratio between the cuboctahedral volume centered on Pb and the octahedral volume.[35] Therefore, some kind of disordered tilting is expected in the region of the depressed $T_{AF} + T_T$ line.

B. The intermediate tilt instability $T_{IT}(x)$ line

The elastic anomaly at T_{IT} satisfies exactly the expectations for the onset of disordered tilting preceding the frustrated LRO tilting: (i) it fills the depression of the $T_{AF} + T_T$ line; (ii) it appears as a steplike softening, similarly to that occurring at T_T for LRO tilting, but spread over a larger temperature range; (iii) it is observed in the elastic but not in the dielectric susceptibility, indicating a nonpolar mode, hence octahedral tilting.

Even though the observation of the anomaly at T_{IT} fits very well in the picture of octahedral tilting, it has not yet been corroborated by diffraction measurements. Actually, superlattice reflections not belonging to the $R3m$ structure are seen in electron diffraction and have been interpreted in terms of in-phase tilts,[36,37] but the composition and temperature range where they are observed is somewhat broader than that enclosed by T_{IT}, making a correlation with T_{IT} questionable. In addition, these in-phase tilts could not be confirmed by x-ray or neutron diffraction and considerable debate ensued over the interpretation of the electron diffraction $\frac{1}{2}\langle 110 \rangle$ spots in terms of AFE $\langle 110 \rangle$ Pb displacements rather than in-phase tilts, due to the much weaker strength of the latter and the greater sensitivity of electron diffraction to the damaged surface.[25,38]

Lacking a confirmation of the nature of the softening at T_{IT} from diffraction experiments, we emphasize the reasons why such an anomaly should indicate some kind of phase transition rather than kinetic effect related to domain walls or defects. There are three features that clearly distinguish the two types of phenomena: (i) cooling causes pinning or freezing of domain walls and therefore decreases the susceptibility, while an increase is observed at T_{IT} (Fig. 4); (ii) in the absence of tilting, the only conceivable walls just below T_C would be between the R-FE domains; if some anomaly in their behavior occurred around T_{IT}, it would appear mainly in the dielectric susceptibility; (iii) the shape of the anomaly is independent of the temperature rate, history, and frequency,[7] and therefore is an intrinsic lattice effect. Following these arguments, we reconfirm the interpretation that the T_{IT} line should correspond to disordered tilting that precedes LRO tilting of the $R3c$ phase below T_T.[7] The new data at low x reveal an unexpected feature: a kink of T_{IT} around $x \sim 0.1$, which we ascribe to cooperative coupling between polar and tilt modes. If octahedral tilts and polar modes were independent of each other, the T_C

and $T_T + T_{IT}$ lines might approach and possibly cross each other in an independent manner. Instead, T_{IT} merges with T_C at $x = 0.06$ with a noticeable kink around $x \sim 0.1$. The T_{IT} line seems "attracted" by T_C, as if the tilt instability were favored by the ferroelectric one. A possible explanation of this observation is in terms of cooperation between a stronger FE instability and a weaker antiferrodistortive tilt instability. The FE mode leaves the lattice unstable also below T_C, since its restiffening is gradual, and also affects the modes coupled to it, in particular favoring the condensation of modes cooperatively coupled to it at a temperature higher than in the normal stiff lattice away from T_C. The rotations of the octahedra are certainly coupled with the polar modes, as demonstrated by the polarization[39,40] and dielectric[7,41] anomalies at the tilt transitions, and a possible mechanism for the merging of two transitions with order parameters (OPs) of different symmetries had been proposed by Holakovský,[42] carried on by Ishibashi.[43] and recently proposed to explain the sequence of phase transitions of the multiferroic BiFeO$_3$.[44] A discussion of the nature of the coupling between tilt and polar modes and the possible consequences in terms of merging of the respective instabilities will be provided elsewhere.[20]

C. The MPB line

The presence of a peak in s' at the MPB has been argued to be evidence that the phase transition occurring at the MPB consists mainly in the rotation of the polarization, from the [001] direction of the T phase toward the [111] direction of the R phase. In fact, in that case the transverse (perpendicular to the original [001] direction) component of P acts as the order parameter and is almost linearly coupled to a shear strain, inducing a peaked response also in the elastic susceptibility.[7,11] This would be an evidence that a monoclinic phase, and not only nanotwinned R and T phases, exists below the MPB. Yet, the smooth shape of the maximum is compatible with an inhomogeneous M phase coexisting and possibly promoted by nanotwinning.[7] In fact, indications continue to accumulate of intrinsic phase heterogeneity near the MPB compositions also on single crystals.[45]

D. Kinks in the T_{MPB} and T_T lines

Other new features of the PZT phase diagram that derive from the present data are the approaches of the $T_{MPB}(x)$ line with T_T and T_C, and a distinct kink in T_T when it encounters T_{MPB}. This is better seen in the detail of the MPB region in Fig. 8, where, besides the same data of Fig. 7, other points of T_{MPB} and T_T are reported from the literature. The data are from diffraction[8] (diamond) piezoelectric coefficient[46] d_{11} (square), $1/s_{11}$ measured with piezoelectric resonance[47] (circle), Raman[9] (—), dielectric ($+$), and infrared ($\times$)[14] spectroscopies, and a combination of dielectric, optical, and diffraction experiments on single crystals.[48]

Let us first consider how $T_T(x)$ enters the MPB region. The points from the literature, obtained from different techniques and samples, are rather sparse, but those from our anelastic and dielectric spectra have little dispersion, and show a clear change of slope of $T_T(x)$ when it approaches T_{MPB} at $0.487 < x < 0.494$. This narrow composition range is close to but not
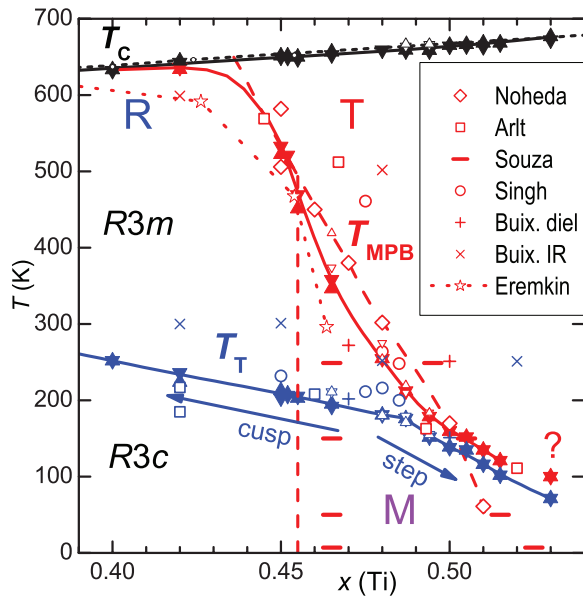
FIG. 8. (Color online) Enlargement of the MPB region of the phase diagram of PZT. Triangles and solid lines from our measurements, as in Fig. 7. Dashed lines and diamonds from Noheda, dotted line and stars from Eremkin, and other open symbols as indicated in the legend. The shape of the continuous $T_{MPB}(x)$ line between $x = 0.42$ and 0.45 is hypothetical.

here as intrinsic of the PZT phase diagram and not vagaries from uncontrolled defects.

It results that also T_T and T_{MPB} almost coincide over an extended composition range, with T_{MPB} seemingly pushed up by T_T. For $x > 0.49$, T_{MPB} deduced from the maximum in s' and T_T deduced from the step in Q^{-1} run parallel and close to each other and it is difficult to assess whether they still represent two distinct transitions or instead they are the manifestations of a same combined polar and tilt transition.

Finally, T_{MPB} seems to join also T_C smoothly; the upper end of the T_{MPB} line in the phase diagrams above is based on only one datum and largely hypothetical but is in line with the much more marked effect observed in single crystals[48] (dotted line in Fig. 8).

The merging of the T_{MPB} with the T_T and perhaps T_C lines prompts considerations similar to those made for the case of T_{IT} and T_C, namely that the coupling between the different modes causes a combined or triggered transition;[42] this will also be discussed in a separate work.[20]

E. Transition in the shape of the Q^{-1} anomaly at T_T: a possible sign of R/M border

As already noted in Sec. IV D, the kink in the T_T line and the transition in the shape of the Q^{-1} anomaly (Fig. 6) appear at slightly different compositions, suggesting that the latter may have a different origin from the proximity to the MPB.

If this were the case, the most obvious explanation for the change of the Q^{-1} anomaly would be the postulated border separating the R and M phases.[8–10] The existence of this border is one of the yet unsettled issues on the phase diagram of PZT, since there are various diffraction studies, also recent and on single crystals,[16,23] whose Rietveld refinements strongly suggest that the R and M phases coexist at least down to $x = 0.4$, so excluding a definite phase border. In addition, according to the view that the M phase is actually a nanotwinned R or T phase,[5,6] this border would not exist. Therefore, an R/M border would be highly significant: It would imply the existence of a LRO M phase. A puzzling feature of this border would be its almost perfect verticality. Indeed, the R/M boundary found by first-principles-based simulations is not vertical: It starts at a triple point with T_C and T_{MPB} at $x_1 = 0.463$ and ends at $T = 0$ and $x_2 = 0.476$.[10] No experimental evidence exists so far of the crossing of such a border with change of temperature, and the change of the shape of the Q^{-1} anomaly between 0.465 and 0.48 is not a conclusive evidence of its existence, since it might be associated with a change of the character of the transition through polarization-tilt coupling near the MPB. Further experiments at more closely spaced compositions are necessary to ascertain this point.

the same over which the anomaly in Q^{-1} changes between cusped and steplike (Fig. 6). In fact that change, marked by arrows in Fig. 8, occurs at $x \lesssim 0.48$, and therefore the two changes may depend on different mechanisms. We will discuss the transition in the shape of the Q^{-1} anomaly in Sec. IV E, and now we focus on the kink in the T_T line, which we think is closely connected with the proximity to the MPB.

In addition, our T_{MPB} points draw a curve with little dispersion, compared to the body of data in the literature, but in this case a difference emerges in the low-temperature region: Even though with only three points below 100 K, the data from diffraction[8] and Raman[9] define an almost straight MPB border that ends at $T = 0$ at $x = 0.520 \pm 0.005$. Instead, our data define a curved line that never crosses T_T. Our closely spaced points in the phase diagram and the regular evolution of the spectra from which they are obtained (Figs. 5 and 6) suggest that the effect is real and characteristic of good quality ceramic samples. The last point with the question mark, obtained from the dashed curve in Fig. 5, probably does not correspond to T_{MPB}, but the difference remains at $x = 0.515$ between our curve at 120 K, and two points at 50–60 K from diffraction and Raman scattering. These discrepancies may depend on differences in the samples rather than on the experimental technique. In fact, the existence of the intermediate monoclinic phase and its nature are not yet unanimously accepted, and it is also proposed that, besides nanoscale twinning, defect structures like planes of O vacancies may have a role in defining the microstructure of PZT and act as nuclei for intermediate phases.[49] Hence, there is a range of microstructures that may well reflect in the position of the MPB, but, again, the consistency and regularity of the data encourage one to consider the features presented

V. CONCLUSIONS

Anelastic and dielectric measurements are reported at compositions of the phase diagram of $PbZr_{1-x}Ti_xO_3$ near the two morphotropic phase boundaries (MPB) of the rhombohedral phase with the tetragonal and the orthorhombic phases. Several new features are found in both regions, provisionally ascribed to octahedral tilting and cooperative coupling between the tilt and polar/antipolar modes.

We provide further evidence in support of the recent proposal[7] of a new phase transition at a temperature T_{IT} that continues the border T_T of the tilt instability up to the Curie temperature T_C, in the region where T_T drops and meets the border with the orthorhombic antiferroelectric phase. The new phase is assumed to represent the initial stage of octahedral tilting, without long-range order due to the enhanced disorder in the cation positions near the AFE border.

The T_{IT} tilt instability line merges with the ferroelectric T_C with an evident step. In addition, the T_T line presents a clear kink when it meets the MPB and, contrary to previous experiments, T_{MPB} is found to deviate and go parallel or even merge with T_T, instead of crossing it. These observations of deviations and merging of tilt and polar instability borders are suggested to arise from cooperative interaction between the polar and the tilt modes.

Another feature that is considered is a rather abrupt transition in the shape of the anomaly in the elastic losses at T_T. The anomaly is a peak or cusp for $x \leqslant 0.465$ and a step for $x \geqslant 0.48$. The possibility is discussed that between these two compositions there is an actual border between rhombohedral and monoclinic phases.

ACKNOWLEDGMENTS

[1] E. Sawaguchi, J. Phys. Soc. Jpn. **8**, 615 (1953).

[2] H. Jaffe, Proc. IEE, Part B: Electron. Commun. Eng. **109**, 351 (1962).

[3] B. Jaffe, W. R. Cook, and H. Jaffe, *Piezoelectric Ceramics* (Academic Press, London, 1971).

[4] B. Noheda, D. E. Cox, G. Shirane, L. E. Cross, and S.-E. Park, Appl. Phys. Lett. **74**, 2059 (1999).

[5] A. G. Khachaturyan, Phil. Mag. **90**, 37 (2010).

[6] K. A. Schönau, L. A. Schmitt, M. Knapp, H. Fuess, Rüdiger-A. Eichel, H. Kungl, and M. J. Hoffmann, Phys. Rev. B **75**, 184117 (2007).

[7] F. Cordero, F. Trequattrini, F. Craciun, and C. Galassi, J. Phys.: Condens. Matter **23**, 415901 (2011).

[8] B. Noheda, D. E. Cox, G. Shirane, R. Guo, B. Jones, and L. E. Cross, Phys. Rev. B **63**, 014103 (2000).

[9] A. G. Souza Filho, K. C. V. Lima, A. P. Ayala, I. Guedes, P. T. C. Freire, F. E. A. Melo, J. Mendes Filho, E. B. Araújo, and J. A. Eiras, Phys. Rev. B **66**, 132107 (2002).

[10] I. A. Kornev, L. Bellaiche, P.-E. Janolin, B. Dkhil, and E. Suard, Phys. Rev. Lett. **97**, 157601 (2006).

[11] F. Cordero, F. Craciun, and C. Galassi, Phys. Rev. Lett. **98**, 255701 (2007).

[12] M. Hinterstein, K. A. Schoenau, J. Kling, H. Fuess, M. Knapp, H. Kungl, and M. J. Hoffmann, J. Appl. Phys. **108**, 024110 (2010).

[13] M. Deluca, H. Fukumura, N. Tonari, C. Capiani, N. Hasuike, K. Kisoda, C. Galassi, and H. Harima, J. Raman Spectr. **42**, 488 (2011).

[14] E. Buixaderas, D. Nuzhnyy, J. Petzelt, L. Jin, and D. Damjanovic, Phys. Rev. B **84**, 184302 (2011).

[15] R. Ranjan, A. K. Singh, Ragini, and D. Pandey, Phys. Rev. B **71**, 092101 (2005).

[16] D. Phelan, X. Long, Y. Xie, Z.-G. Ye, A. M. Glazer, H. Yokota, P. A. Thomas, and P. M. Gehring, Phys. Rev. Lett. **105**, 207601 (2010).

[17] R. S. Solanki, A. K. Singh, S. K. Mishra, S. J. Kennedy, T. Suzuki, Y. Kuroiwa, C. Moriyoshi, and D. Pandey, Phys. Rev. B **84**, 144116 (2011).

[18] F. Cordero, L. Dalla Bella, F. Corvasce, P. M. Latino, and A. Morbidini, Meas. Sci. Technol. **20**, 015702 (2009).

[19] A. S. Nowick and B. S. Berry, *Anelastic Relaxation in Crystalline Solids* (Academic Press, New York, 1972).

[20] F. Cordero, F. Trequattrini, F. Craciun, and C. Galassi, arXiv:1208.1618.

[21] W. Rehwald, Adv. Phys. **22**, 721 (1973).

[22] M. A. Carpenter and E. H. K. Salje, Eur. J. Mineral. **10**, 693 (1998).

[23] H. Yokota, N. Zhang, A. E. Taylor, P. A. Thomas, and A. M. Glazer, Phys. Rev. B **80**, 104109 (2009).

[24] N. Zhang, H. Yokota, A. M. Glazer, and P. A. Thomas, Acta Cryst. B **67**, 386 (2011).

[25] D. I. Woodward, J. Knudsen, and I. M. Reaney, Phys. Rev. B **72**, 104110 (2005).

[26] I. D. Brown, Acta Cryst. B **48**, 553 (1992).

[27] I. D. Brown, A. Dabkowski, and A. A. McCleary, Acta Cryst. B **53**, 750 (1997).

[28] H. D. Megaw, Proc. Royal Soc. **58**, 133 (1946).

[29] P. M. Woodward, Acta Cryst. B **53**, 44 (1997).

[30] I. M. Reaney, E. L. Colla, and N. Setter, Jpn. J. Appl. Phys. **33**, 3984 (1994).

[31] R. J. Angel, J. Zhao, and N. L. Ross, Phys. Rev. Lett. **95**, 025503 (2005).

[32] A. M. Glazer, Acta Cryst. B **28**, 3384 (1972).

[33] Ragini, S. K. Mishra, D. Pandey, H. Lemmens, and G. VanTendeloo, Phys. Rev. B **64**, 054101 (2001).

[34] D. M. Hatch, H. T. Stokes, R. Ranjan, Ragini, S. K. Mishra, D. Pandey, and B. J. Kennedy, Phys. Rev. B **65**, 212101 (2002).

[35] D. Wang and R. J. Angel, Acta Cryst. B **67**, 302 (2011).

[36] D. Viehland, Phys. Rev. B **52**, 778 (1995).

[37] D. Viehland, J.-F. Li, X. Da, and Z. Xu, J. Phys. Chem. Sol. **57**, 1545 (1996).

[38] J. Ricote, D. L. Corker, R. W. Whatmore, S. A. Impey, A. M. Glazer, J. Dec, and K. Roleder, J. Phys.: Condens. Matter **10**, 1767 (1998).

[39] R. W. Whatmore, R. Clarke, and A. M. Glazer, J. Phys. C: Solid State Phys. **11**, 3089 (1978).

[40] N. Cereceda, B. Noheda, T. Iglesias, J. R. Fernandez-del-Castillo, J. A. Gonzalo, N. Duan, Y. L. Wang, D. E. Cox, and G. Shirane, Phys. Rev. B **55**, 6174 (1997).

[41] X. Dai, Z. Xu, J.-F. Li, and D. Viehland, J. Appl. Phys. **77**, 3354 (1995).

[42] J. Holakovský, Phys. Stat. Sol. (b) **56**, 615 (1973).

[43] Y. Ishibashi, J. Phys. Soc. Jpn. **63**, 2082 (1994).

[44] I. A. Kornev and L. Bellaiche, Phys. Rev. B **79**, 100105 (2009).

[45] R. G. Burkovsky, Yu. A. Bronwald, A. V. Filimonov, A. I. Rudskoy, D. Chernyshov, A. Bosak, J. Hlinka, X. Long, Z.-G. Ye, and S. B. Vakhrushev, Phys. Rev. Lett. **109**, 097603 (2012).

[46] G. Arlt, in *IEEE Ultrasonic Symposium* (IEEE, Washington, DC, 1990), p. 733.

[47] A. K. Singh, S. K. Mishra, Ragini, D. Pandey, S. Yoon, S. Baik, and N. Shin, Appl. Phys. Lett. **92**, 022910 (2008).

[48] V. V. Eremkin, V. G. Smotrakov, and E. G. Fesenko, Sov. Phys. Solid State **31**, 1002 (1989).

[49] L. A. Reznichenko, L. A. Shilkina, O. N. Razumovskaya, E. A. Yaroslavtseva, S. I. Dudkina, O. A. Demchenko, Yu. I. Yurasov, A. A. Esis, and I. N. Andryushina, Phys. Solid State **51**, 1010 (2009).